RESEARCH ARTICLE

Altered coupling between resting-state glucose metabolism and functional activity in epilepsy

Jingjuan Wang[1], Yi Shan[2,3], Jindong Dai[4,5], Bixiao Cui[1], Kun Shang[1], Hongwei Yang[1], Zhongwei Chen[6], Baoci Shan[7,8,9], Guoguang Zhao[10] & Jie Lu[1,2,3]

[1]Department of Nuclear Medicine, Xuanwu Hospital Capital Medical University, Beijing, China
[2]Department of Radiology, Xuanwu Hospital Capital Medical University, Beijing, China
[3]Key Laboratory of Magnetic Resonance Imaging and Brain Informatics, Beijing, China
[4]Department of Neurosurgery, Beijing Haidian Section of Peking University Third Hospital, Beijing, China
[5]Department of Functional Neurosurgery, Xuanwu Hospital Capital Medical University, Beijing, China
[6]GE Healthcare, Beijing, China
[7]Division of Nuclear Technology and Applications, Institute of High Energy Physics, Chinese Academy of Sciences, Beijing, China
[8]Beijing Engineering Research Center of Radiographic Techniques and Equipment, Beijing, China
[9]CAS Centre for Excellence in Brain Science and Intelligent Technology, Shanghai, China
[10]Department of Neurosurgery, Xuanwu Hospital, Capital Medical University, Beijing, China

Correspondence

Jie Lu, No.45 Changchun Street, Xicheng District, 100053, Beijing, China. Tel: +8610-8319-8379; Fax: +86 10 83198379; E-mail: imaginglu@hotmail.com
Guoguang Zhao, No.45 Changchun Street, Xicheng District, 100053, Beijing, China. Tel: +8610-8319-8252; Fax: +86 10 63012833; E-mail: ggzhao@vip.sina.com

Abstract

Objective: Altered functional activities and hypometabolism have been found in medial temporal lobe epilepsy patients with hippocampal sclerosis (mTLE-HS). Hybrid PET/MR scanners provide opportunities to explore the relationship between resting-state energy consumption and functional activities, but whether repeated seizures disturb the bioenergetic coupling and its relationship with seizure outcomes remain unknown. **Methods**: ^{18}F-FDG PET and resting-state functional MRI (rs-fMRI) scans were performed with hybrid PET/MR in 26 patients with mTLE-HS and in healthy controls. Energy consumption was quantified by ^{18}F-FDG standardized uptake value ratio(SUVR) relative to cerebellum. Spontaneous neural activities were estimated using regional homogeneity (ReHo), fractional amplitude of low frequency fluctuations (fALFF) from rs-fMRI. Between-group differences in SUVR and rs-fMRI derived metrics were evaluated by two-sample t test. Voxel-wise spatial correlations were explored between SUVR and ReHo, fALFF across gray matter and compared between groups. Furthermore, the relationships between altered fALFF/SUVR and ReHo/SUVR coupling and surgical outcomes were evaluated. **Results**: Both the patients and healthy controls showed significant positive correlations between SUVR and rs-fMRI metrics. Spatial correlations between SUVR and fMRI-derived metrics across gray matter were significantly higher in patients with mTLE-HS compared with healthy controls (fALFF/SUVR, $P < 0.001$; ReHo/SUVR, $P = 0.022$). Higher fALFF/SUVR couplings were found in patients who had Engel class IA after surgery than all other ($P = 0.025$), while altered ReHo/SUVR couplings ($P = 0.097$) were not. **Conclusion**: These findings demonstrated altered bioenergetic coupling across gray matter and its relationship with seizure outcomes, which may provide novel insights into pathogenesis of mTLE-HS and potential biomarkers for epilepsy surgery planning.

Introduction

Medial temporal lobe epilepsy (mTLE-HS) is a common type of refractory epilepsy in adults, characterized by repeated seizures originating from hippocampus and related mesial temporal lobe structures.[1] EEG studies have found extensively abnormal discharge in cortical and subcortical brain regions, which are associated with seizure

generation and propagation. So mTLE-HS is thought to be a network disease, in which the hippocampus is a key component. It is thus important to better clarify the brain functional networks changes for pathogenesis of mTLE-HS.

Previous studies have investigated spontaneous intrinsic activities in mTLE-HS using fractional amplitude of low-frequency fluctuations (fALFF) and regional homogeneity (ReHo) with Resting state functional MRI (rs-fMRI). fALFF estimates the amplitude of spontaneous neural activities for a single voxel.[2] ReHo measures the degree of local synchronization between the time series of a given voxel and its nearest neighbours.[3] Increased fALFF of the mesial temporal lobe, thalamus, and a few of other cortical and subcortical structures was discovered in TLE patients compared to the healthy control.[4] Significantly increased ReHo was distributed in ipsilateral parahippocampal gyrus, midbrain, insula, corpus callosum, bilateral sensorimotor cortex, and fronto-parietal subcortical structures.[5] Furthermore, increased fALFF and ReHo in these regions were found to be related with epileptic activities. There was a strong concordance between regions with increased ALFF and ReHo with the epileptic networks in patients with mTLE-HS. Decreased fALFF and ReHo were found in default mode network, into which epileptic activity may spread from temporal lobe. In parallel, glucose metabolic changes in epilepsy could be routinely observed as low signals with in vivo ^{18}F-FDG-PET imaging in the temporal and extratemporal areas, which also showed a significant overlap between hypometabolism and EEG epileptic networks.[6] Hypermetabolism areas partly coincided with the default mode network. Metabolism changes in these regions can be used to predict seizure outcomes and correlated with clinical characteristics, including seizure onset and the epilepsy duration.[7]

The previous fMRI and ^{18}F-FDG PET studies have reported disrupted intrinsic activity and metabolism in mTLE-HS. However, there is still a lack of comprehensive analysis about the relationship between intrinsic activity and metabolism in brain networks. Tomasi et al have reported that higher glucose metabolism was associated with proportionally larger MRI signal amplitudes in the brain.[8] The underlying bioenergetics coupling may be fundamental for effective neural signaling and interneuronal communication. Because bioenergetics coupling, characterized by correlation between the spontaneous neural activities and energy consumption, need to be only detected by investigating the spontaneous neural activities and energy consumption simultaneously.[9-10] Until now, only few studies attempted to investigate whether the relationship are preserved in subjects with TLE.

The recent emergence of hybrid PET/MR scanners allows a simultaneous acquisition of images reflecting metabolic and functional activities.[11] The research in healthy controls has identified a significant correlation of the spatial distribution between standardized uptake value ratio (SUVR) and rs-fMRI derived metrics at different scales using a hybrid PET/MR scanner,[12] while the weaker correlation has been found significantly in Alzheimer disease patients in another study.[13] However, it remains unknown whether the repeated seizures could disturb the underlying bioenergetics coupling in patients with mTLE-HS.

We hypothesized that the altered coupling between the brain intrisic activities and energy consumption was found in the patients with mTLE-HS. In this study, we analyzed abnormal intrisic activities and energy consumption, spatial correlations between the rs-fMRI derived metrics and SUVR with hybrid PET/MR data and further investigated the relationship between altered couplings and surgical outcomes.

Materials and Methods

Participants

35 patients with refractory mTLE-HS were recruited in this prospective study from March 2016 to May 2018. All patients were admitted by the Neurology Department of Xuanwu Hospital, Capital Medical University (Beijing, China). Subsequently, the standard anterior temporal lobectomy was performed in these patients. 30 healthy controls were recruited in local community. The patients with mTLE-HS were undergone comprehensive clinical evaluation including semiology, interictal and ictal scalp EEGs, structural MRI, and histopathological results, according to ILAE diagnostic methods.[14] The inclusion criteria for patients were as follows: typical symptoms of mTLE, pure unilateral hippocampal sclerosis, epileptic spikes in the unilateral frontotemporal or temporal lobes, no seizure for at least 72 hours before PET/MR imaging. The exclusion criteria for all participants were: previous brain surgery, drug abuse, other chronic neurological disease or other psychiatric disorders, any contraindications for MRI, and incomplete MRI or PET data. Nine patients and four healthy controls were excluded based on exclusion criteria: contraindications for MRI (2 of 35), incomplete fMRI or PET data in the same subject (2 of 35 and 1 of 30), other chronic neurological disease (5 of 35 and 3 of 30).

Finally, 26 patients with refractory mTLE-HS were included in this study. Of which, 24 had annual postoperative visits to perform evaluation of surgical outcomes by the Engel Epilepsy Surgery Outcome Scale,[15] while two patients failed to follow-up with their recorded contact information. Of this 12 patients were completely seizure-

free (Engel class IA), 8 patients were nondisabling simple partial seizures (Engel class IB), 2 patients have almost seizure free (Engel class Ⅱ), and 2 patients have worthwhile improvement (Engel class Ⅲ). 26 healthy controls were included in control group. The demographic and clinical characteristics of all participants are summarized in Table 1.

The protocol of this study was approved by the Ethics committee of Xuanwu Hospital. A written informed consent was obtained for each participant prior to the procedure.

Data acquisition

All images were acquired simultaneously during the interictal stage with resting state using a hybrid TOF-PET/MR scanner (SIGNA, GE Healthcare, WI, USA). PET and MR data were obtained simultaneously with the same scanning center to ensure the precise fusion and registration of multi-modality imaging. Patients guarantee seizure free status in at least 72 hours preceding PET/MR imaging. All scanning was performed in a dimmed environment. Additionally, standard earplugs and headphones were used to avoid noise interference. During the scanning, subjects were instructed to keep their eyes open, avoid focusing their mind on anything, and keep their head as still as possible. After a bolus injection of 3.7MBq/kg ^{18}F-FDG tracer, BOLD fMRI, 3D ASL, 3D T1 BRAVO, and DTI

were immediately scanned, followed by structural imaging sequences for diagnosis. At 30 minutes post-injection, saturated list mode PET data corresponded with BOLD fMRI were recorded for 10 minutes and reconstructed with Ordered Subsets Expectation Maximization algorithm (8 iterations and 32 subsets, 3mm cut-off). Attenuation correction, scatter correction, random correction, and dead-time correction were performed as well. Scanning parameters were as follows for reconstructed images: matrix size = 192 * 192, voxel size = 1.82 * 1.82 * 2.78mm^3, 89 slices; for rs-fMRI imaging (EPI):TR = 2000ms, TE = 30ms, flip angle = 90°, FOV read = 192 mm, matrix size = 64*64, voxel size = 3.0 * 3.0 * 3.0 mm^3, lasted for 10 minutes; for structural imaging (MP-RAGE): TR = 2300 ms, TE = 2.98 ms, angle = 9°, 160 slices with 0.5mm gap, FOV read = 256 mm, matrix size = 256 * 256, voxel size = 1.0 * 1.0 * 1.0 mm^3.

Data analysis

All imaging data were preprocessed in SPM12 (http://www.fil.ion.ucl.ac.uk/spm/software/spm12) and an in-house code in Matlab. PET images and fMRI images of 12 patients with left hippocampal sclerosis were left–right flipped for further data analysis, ensuring a homogeneous group with epileptogenic zone of patients on the same side. For voxel wise analysis of multimodal dataset, all individual maps were registered with corresponding high resolution T1 images, and spatially normalized to the Montreal Neurological Institute (MNI) by the same transformation parameters. The transformations were derived from the segmentation procedure of high resolution T1 weighted images. Then, spatial distribution similarity and spatial correlation were analyzed among co-registered multimodal maps. Detailed information was outlined as follows.

T1 data

Structural images were skull-stripped, segmented into gray matter, white matter and cerebrospinal fluid using Dartel toolbox on SPM12. Gray matter segments were modulated by Jacobian of the nonlinear transformation of coordinates for gray matter volume. Structural images were also aligned to fMRI and FDG PET images, and then segmented into gray matter, white matter, and cerebrospinal fluid. The forward transformation was derived from the segmentation procedure for spatially normalizing fMRI and FDG PET images to MNI space. Individual GM binary masks were thus derived by thresholding (>0.5) the gray matter probability images of individual subject. The following individual analysis was performed in this mask.

Table 1. The demographics and clinical features in all participants

Characteristics	mTLE (n = 26)	HC (n = 26)	P value
Age (years,mean ± SD)	28.86 ± 6.99	29.31 ± 6.42	0.81[a]
Gender(M/F)	12/14	16/10	0.202[b]
Age at onset(years, mean ± SD)	16.00 ± 8.86		
Disease duration(years, mean ± SD)	11.48 ± 5.87		
Side (L/R)	12/14		
Family history of epilepsy (%)	0 (0%)		
History of febrile convulsion	2 (7.69%)		
History of viral encephalitis	2 (7.69%)		
Types of anticonvulsants			
≥3	10 (38.46%)		
Seizure Frequency			
Daily	4 (15.38%)		
weekly	7 (26.92%)		
Monthly	9 (34.62%)		
Yearly	6 (23.08%)		

Values are expressed as a mean ± standard deviation. mTLE, Medial temporal lobe epilepsy; HC, healthy controls; a, two-sample t test; b, Chi-square test.

PET data

^{18}F-FDG-PET images were skull-stripped using Brain Extraction Tool. To control for potential partial volume effects on PET images, a voxelwise partial volume correction (PVC) was applied to ^{18}F-FDG-PET images using PETPVE12 toolbox based on SPM12.[16] Individual partial volume corrected PET data were coregistered with corresponding T1 weighted images, and then spatially normalized to the MNI template using the spatial transformation parameters from segmentation procedure. Preprocessed PET images in MNI space were converted to standardized uptake value ratio (SUVR) relative to cerebellum and then smoothed using 6-mm full width at half maximum (FWHM) gaussian kernel. Regional SUVR was extracted on the ^{18}F-FDG SUVR images.

fMRI data

As previous studies described, after discarding 10 first volumes, fMRI data were realigned, registered with individual T1 weighted images, normalized to MNI space using the spatial transformation parameters from the SPM12 unified segmentation algorithm and smoothed (Gaussian kernel 8*8*8 mm^3) in Data Processing & Analysis for (Resting-State) Brain Imaging (https://www.nitrc.org/projects/dpabi/).[17] fALFF maps, which measured the relative contribution of low frequency range (0.01-0.1H$_Z$) to the whole frequency range of signal oscillations, were computed. Then temporally bandpass filtering (0.01-0.1Hz) was performed to reduce higher frequency and physiological noise. ReHo, examined the degree of regional coherence of 27 neighboring voxels, was calculated after temporal filtering as well. Besides, spatial smoothing (FWHM = 6 mm) was also performed before fALFF calculation, but after ReHo and DC.

Statistical analysis

The bilateral hippocampal volume was extracted by multiplying the hippocampus mask from the WFU PickAtlas tool. The masks overlie in T1 weighted images were showed in Supplementary Figure S1A. For each imaging metric, two sample t-tests were performed to estimate group differences after controlling for age, gender, and the ipsilateral hippocampus volume. Multiple comparisons were performed using Monte Carlo simulations in the DPABI. SUVR, fALFF, and ReHo in bilateral hippocampus were extracted and assessed differences between hemispheres using paired t tests and between patient group and healthy control group using two sample t tests.

To assess the coupling between glucose metabolism and spontaneous neural activities in patients with mTLE-HS, standardized SUVR, ReHo, and fALFF maps into Z values with respect to mean and standard deviation across the individual's gray matter mask and calculated subject-special Spearman's correlation coefficient correlation (partial correlation) based on the partial volume corrected PET images. Group differences of correlation between SUVR and rs-fMRI derived metrics were evaluated by two sample t tests. $P < 0.05$ was treated as statistically significant.

Finally, Pearson correlation analysis was used to investigate the relationship between the intermodalities correlation and clinical characters, age of onset, duration of illness, seizure frequency. We further evaluated the differences of the intermodalities correlation between Engel class IA and all others using two sample Students t-tests with a threshold of significance set at $P < 0.05$.

Results

Spatial distribution of the SUVR, ReHo and fALFF

Similar spatial distribution in the whole brain was observed visually in mean SUVR and rs-fMRI derived metrics maps of two groups (Fig. 1). Both patients and control groups largely exhibited higher glucose metabolism in precuneus, medial prefrontal cortex, middle frontal gyrus, medial temporal, and parietal cortices that comprised the default mode network (DMN), and in the lateral temporal cortex, insula and sensorimotor cortex. Brain regions with higher fALFF/ReHo were mostly located in the occipital gyrus, the DMN, and sensorimotor cortex. Our above results also showed that the PVC could remarkably improve spatial resolution and contrast. The following results focused on partial volume corrected SUVR.

Between group difference among SUVR, ReHo and fALFF

Significant gray matter atrophy of ipsilateral hippocampus was showed in patients compared with controls ($P < 0.001$), while no significant differences were found in contralateral hippocampus ($P = 0.379$, Supplementary Fig. S1). Controlling for age, sex, and ipsilateral hippocampus volume, patients showed significant ^{18}F-FDG hypometabolism mainly on the affected side, involving the temporal cortex, hippocampus, middle frontal cortex, thalamus, insula, postcentral gyrus in contrast with control groups (Fig. 2A,B).

In general, all rs-fMRI metrics exhibited lower fALFF/Reho in default mode network and cerebellum compared with the controls. Higher fALFF was mainly located in
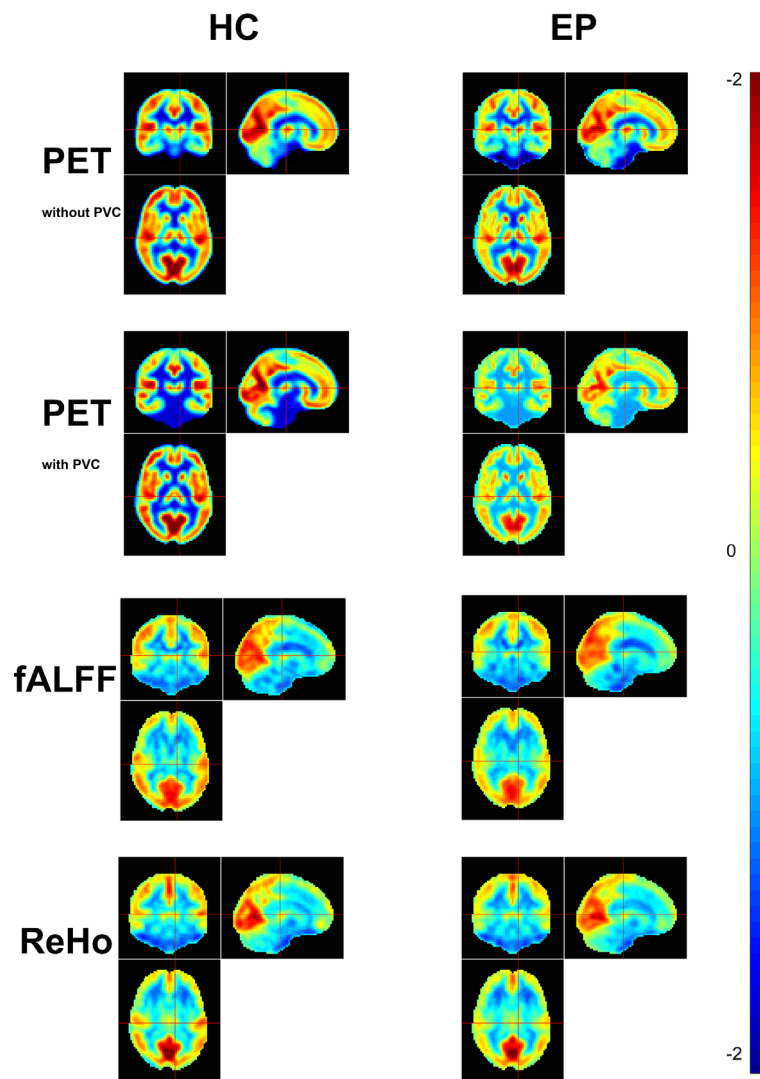
Figure 1. Spatial distribution maps of SUVR, fALFF, and ReHo in patient and HC groups. The maps are normalized to the MNI space and averaged across subjects within groups. Z-scores in all images are scaled to the same range. ^{18}F-FDG SUVR images with PVC and without PVC were all showed. HC, healthy controls; fALFF, fractional amplitude of low frequency fluctuations; L, left; mTLE-HS, medial temporal lobe epilepsy patients with hippocampal sclerosis; R, right; ReHo, regional homogeneity; SUVR, standardized uptake value ratio; PVC, partial volume correction.

the bilateral medial temporal lobe, orbital part of inferior frontal lobe, anterior and middle cingulate cortex, and insula in nonaffected side. Higher ReHo was seen in bilateral inferior temporal lobe, hippocampus, parahippocampal gyrus, mygdala in the affected side, postcentral lobe in nonaffected side (Fig. 2C,D).

Finally, we compared the SUVR, fALFF, and ReHo in the hippocampus between hemispheres and between groups. Significant hypometabolism in ipsilateral hippocampus was found compared with either contralateral hippocampus in patients or ipsilateral hippocampus in healthy controls. There was significant decreased fALFF in ipsilateral hippocampus compared with contralateral

hippocampus in patients, while there was no statistically significant decreased fALFF compared with healthy controls. Significant decreased ReHo was found in bilateral hippocampus compared with healthy controls.

Across voxel wise coupling among SUVR, ReHo, and fALFF

Each subject showed significant Spearman correlations between ^{18}F-FDG-PET and rs-fMRI metrics across gray matter. Figure 3 shows the representative scatter plots of spatial correlations between ^{18}F-FDG-PET and rs-fMRI metrics from two participants (a healthy subject, woman,
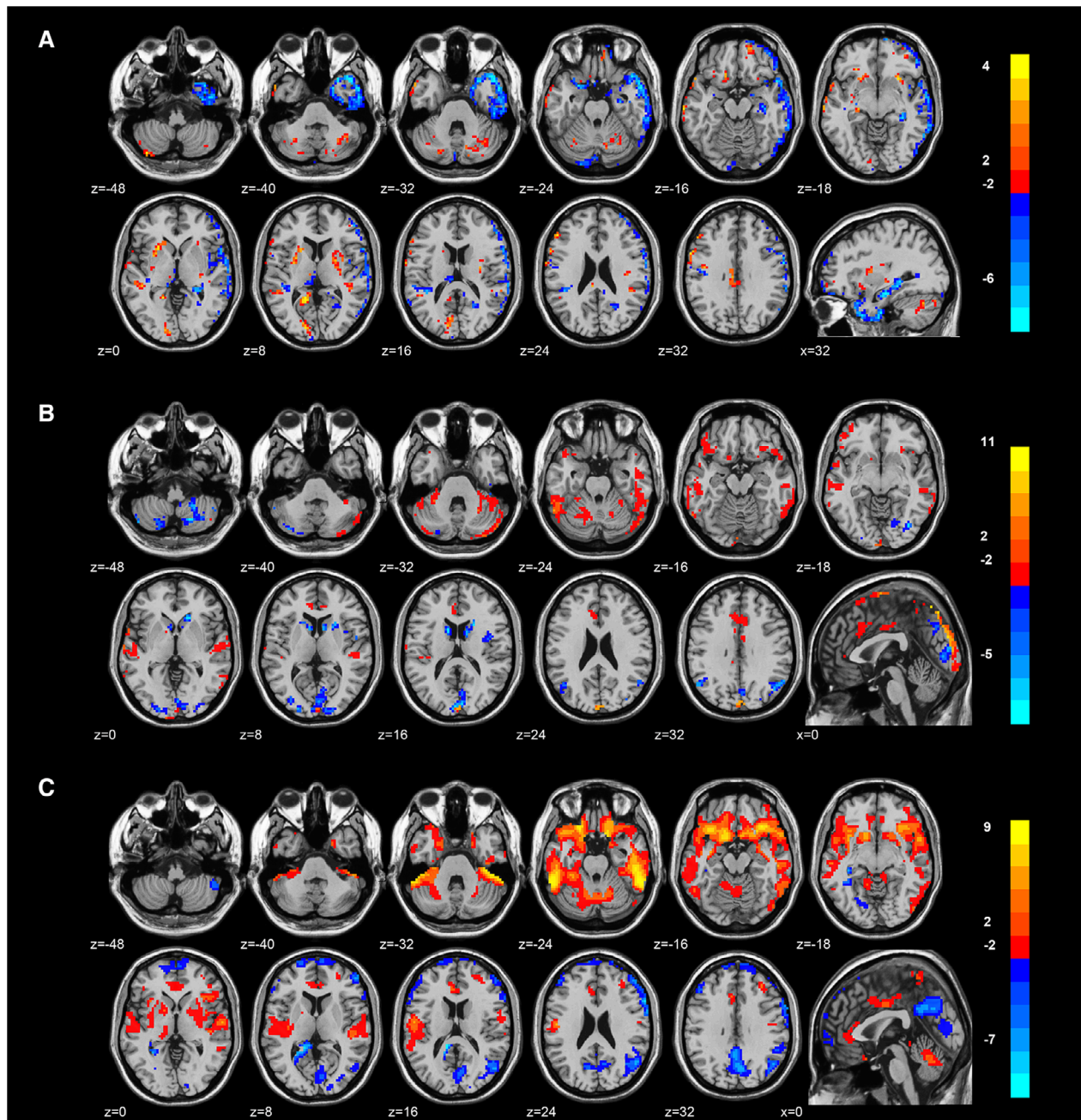
Figure 2. Brain regions with significant group differences in (A) SUVR, (B) fALFF, and (C) ReHo in patients, compared with healthy controls groups. A significantly increase of all variables in patient group are found in regions in warm color. Regions in cold color have a significantly decrease in patient group. To ensuring a homogeneous group with all patients having the epileptogenic zone on the same side, images of 12 patients with left hippocampal sclerosis were left-right reversed to lateralize the epileptogenic side to the right for all patients. Right is displayed on the right (neurological convention). fALFF, fractional amplitude of low frequency fluctuations; ReHo, regional homogeneity; SUVR, standardized uptake value ratio.

age = 40 years old, and a patient with mTLE-HS, man, age = 32 years old).

The correlation coefficients were summarized as means and standard deviations for each group. Regarding the

fALFF/SUVR relationship, Spearman correlation coefficients were significantly higher in patients with mTLE-HS than healthy controls (healthy controls, 0.44 ± 0.12; patients with mTLE-HS, 0.51 ± 0.08; p = 0.022, Fig. 4). While patients
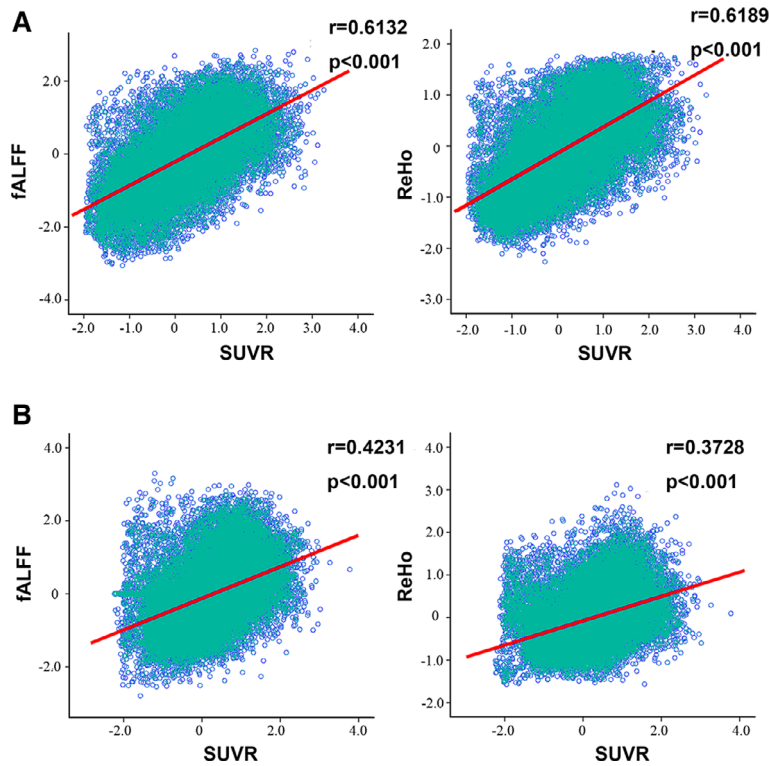
Figure 3. Representative scatter plots of pair-wise spatial correlations between SUVR and fALFF, ReHo over voxels belonging to the ipsilateral hippocampal network. (A) a patient (man, age = 32 years old, disease duration = 15 years, seizure frequency = 3-4times/month) and (B) a healthy subject (woman, age = 30 years old), fALFF, fractional amplitude of low frequency fluctuations; ReHo, regional homogeneity, SUVR, standardized uptake value ratio.

have higher correlation coefficients of ReHo/SUVR than healthy controls (healthy controls, 0.44 ± 0.10; patients with mTLE-HS, 0.53 ± 0.07; $P < 0.001$, Fig. 4).

Correlations between the intermodalities correlation and clinical parameters

We did not find significant correlations between epilepsy duration, seizure frequency, and the intermodalities

coupling. Furthermore, the correlations between the intermodalities coupling and Engel classification were estimated in 24 patients with successful postoperative visits. Higher fALFF/SUVR correlates the less postoperative seizure. The fALFF/SUVR correlation decreased along with worse outcomes. Results showed significant differences in the fALFF/SUVR coupling between two outcome groups ($P = 0.025$ for Engel IA vs. Engel IB-III, Fig. 5), but no significant differences in the ReHo/
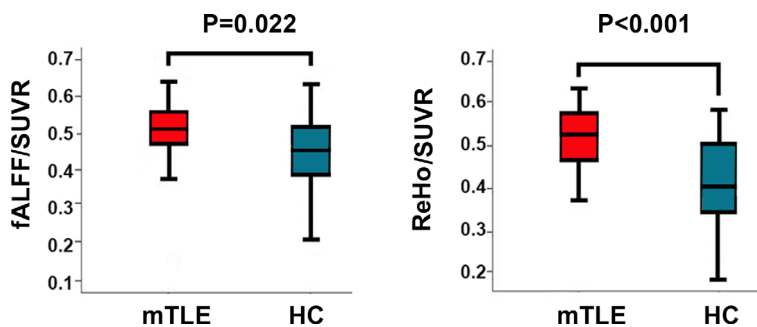

Figure 4. Spatial correlations between SUVR and fALFF, ReHo across gray matter with significant group differences between groups. Patients show significantly increased spatial correlations compared to controls (fALFF/SUVR, $P = 0.022$; ReHo/SUVR, $P < 0.001$). HC, healthy controls; fALFF, fractional amplitude of low frequency fluctuations; ReHo, regional homogeneity; SUVR, standardized uptake value ratio.
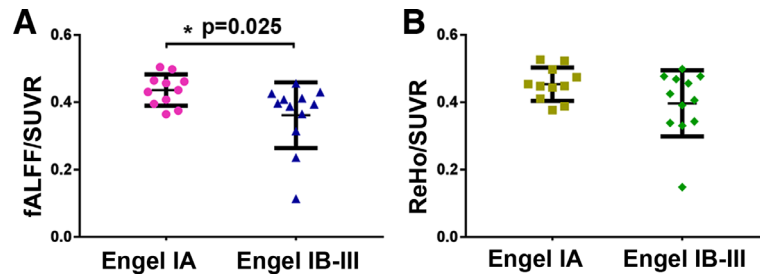
Figure 5. Resting-state FDG/fMRI correlations within gray matter voxels in individual patient. fALFF/SUVR correlation(A) and fALFF/SUVR correlation(B) are shown for patients who were seizure free (Engel class IA) after surgery and all others (Engel class IB to IV). Higher fALFF/SUVR couplings were found in patients who had Engel class IA after surgery than all other ($P = 0.025$), while altered ReHo/SUVR couplings ($P = 0.097$) were not. ReHo, regional homogeneity; fALFF, fractional amplitude of low frequency fluctuations, SUVR, standardized uptake value ratio. P values are given for group differences.

SUVR coupling ($P = 0.097$ for Engel IA vs. Engel IB-III, Fig. 5).

Discussion

The current study investigated the coupling changes between brain metabolism and functional activities in patients with mTLE-HS by simultaneous rs-fMRI and ^{18}F-FDG-PET. We found that both the patients with mTLE-HS and healthy controls showed significant positive correlations between the SUVR and rs-fMRI metrics across gray matter. Specifically, patients with mTLE-HS have higher positive correlations than healthy controls in both fALFF/SUVR and ReHo/SUVR coupling. Importantly, altered fALFF/SUVR coupling was associated with postoperative seizure outcomes. These results provided direct evidence for altered bioenergetic coupling and its relationship with seizure outcome in mTLE-HS, which may improve the understanding of the pathogenesis of mTLE-HS and provide potential noninvasive markers for predictive of postoperative seizure outcomes.

Previous stand-alone studies have investigated metabolic and intrinsic activity changes in mTLE-HS.[18] In a good agreement with these findings, our results also showed that both FDG PET and fMRI metrics could differentiate mTLE-HS patients from healthy controls. The regions showing hypometabolism, increased fALFF and ReHo are usually involved in generation and propagation of epileptiform activity. While the regions showing hypermetabolism, decreased ALFF and ReHo are partly located in the areas of default-mode network. Although these findings regarding metabolism and rs-MRI metrics (metabolism decreased, rs-fMRI metrics increased) seem to be opposite, it is reasonable because of different physiological mechanism. Hypometabolism may be due to neuronal cell loss of focal lesion,[19] and failure of inhibition processes in propagation pathways.[6] A surround inhibition would be generated due to focal seizure activity to limit the spread of ictal

discharges. Once the inhibition processes failed, ictal discharges spread via the anatomic pathways and further facilitated by a lack of inhibition to constitute larger epileptic network.[6] The same with hypometabolism, increased ALFF and ReHo were not confined to focal brain areas, but comprised temporal epileptic network reported by intracranial EEG studies. The increased ALFF/ReHo may be due to increased spikes of epileptic neurons and related to interictal epileptic activity in epileptic network.[4]

In line with previous studies, we found significant across voxels couplings between the glucose metabolism and fALFF, ReHo in healthy controls group.[20] These findings indicate an intact neuronal vascular networks, in which brain regions with higher spontaneous neuronal activity tend to have greater metabolic demand. Patients with mTLE-HS also showed significant across voxel coupling between the glucose metabolism and fALFF, ReHo. Specially, a significantly increased coupling between the glucose metabolism and fALFF, ReHo was found in mTLE-HS compared with healthy controls. However, previous non-simultaneous resting-state ^{18}F-FDG-PET/fMRI study showed no significant correlation between brain metabolism and ReHo within gray matter.[12] There may be two possible reasons for this discrepancy. First, we guaranteed the coupling of the brain activity represented by the two techniques using simultaneous PET/MR. Second, the patients is not homogeneous. In the previous study, there were significant metabolic changes in the hippocampus of mTLE-HS patients between hemispheres, but there were no differences between groups. In this study, we evaluated neurodegeneration in hippocampus by regional gray matter volume and SUVR. All the results confirmed that gray matter volume and metabolism in hippocampus differed between hemispheres and between groups.

Epileptic discharges were assumed to be an "external task", inducing task-related activities.[4] The relationship between the rs-fMRI derived metrics and glucose metabolism under activation conditions had been investigated.

Table 2. Group differences in (A) SUVR, (B) fALFF, and (C) ReHo in patients, compared with healthy controls groups

	Cluster size	Regions	MNI			T
SUVR EP<HC	2204	Temporal_Inf_R Temporal_Mid_R Insula_R	36	9	−45	−7.8333
	127	Hippocampus_R ParaHippocampal_R	33	−18	−18	−6.6746
	421	Frontal_Mid_R	42	36	−21	−5.56
	247	Putamen_L	−24	9	−24	−5.931
	64	Thalamus_L	−9	−27	12	−4.8849
	56	Precuneus_R	24	−60	24	−3.955
	67	Postcentral_R	9	−39	57	−4.0274
EP>HC	105	Left Cerebellum	−39	−78	−48	5.26
	159	Left Cerebellum	33	−66	−30	4.0854
	56	Precuneus_L Cingulum_Post_L	−15	−51	9	5.9736
	44	Occipital_Sup_L	−15	−87	6	5.3123
fALFF						
EP>HC	204	Temporal_Inf_R	27	−45	−30	5.7637
	289	Temporal_Mid_L Temporal_Inf_L	−51	−48	−27	5.7535
	214	Cingulum_Mid_L Cingulum_Ant_L	−6	−12	39	5.7063
	81	Frontal_Inf_Orb_L	−36	48	−12	3.6573
	43	Frontal_Inf_Orb_R	30	27	−18	3.5808
	85	Temporal_Sup_R	54	−15	0	3.2553
EP<HC	164	Cerebelum_8_R	18	−63	−51	−5.3439
	149	Cerebelum_8_L	−12	−54	−57	−5.7291
	59	Angular_L	−51	−60	33	−3.7756
	94	Angular_R	54	−60	36	−3.7198
ReHo						
EP>HC	233	Temporal_Inf_L Temporal_Mid_L ParaHippocampal_L	−57	−45	−27	9.4947
	350	Temporal_Inf_R Insula_R Frontal_Inf_Orb_R	54	−42	−27	9.5856
	57	Postcentral_L Rolandic_Oper_L	−54	−9	18	5.3849
	49	Fusiform_L	−27	−21	−27	2.9618
	28	Hippocampus_R Amygdala_R ParaHippocampal_R	24	−3	−21	3.2778
EP<HC	109	Cingulum_Mid_L	−6	−15	36	−5.1183
	44	Thalamus_L	−6	−18	18	−7.1457
	30	Thalamus_R	9	−18	18	−6.1967
	88	Temporal_Mid_R Angular_R	51	−63	27	−4.5447
	82	Frontal_Sup_L	−18	39	54	−5.3442
	80	Angular_L	−42	−72	42	−4.5872
	14	Insula_R	45	−27	24	−5.0318
	24	Precentral_R	63	18	24	−4.6644
	71	Precuneus_R	6	−72	36	−4.8332
	48	Precuneus_L	−6	−45	51	−3.6827

During visual stimulation, a stronger voxel-wise spatial relationship between the changes in BOLD synchronization and glucose uptake in activated brain regions had been shown using a hybrid PET/MR.[21-22] Similarly, the relationship between degree centrality and cerebral blood flow strengthened with increasing task load during an N-

Table 3. Mean z values for SUVR, fALFF, and ReHo in bilateral hippocampus and correlations among these three metrics

	TLE: Ipsilateral Hippocampus Mean(std)	HC: Right Hippocampus Mean(std)	P	TLE: Contralateral Hippocampus Mean(std)	HC: Left hippocampus Mean(std)	P
SUVR	−0.323 (0.159)[a]	−0.059 (0. 100)[a]	<0.001[bc]	0.068 (0.265)[a]	0.041 (0.100)[a]	0.627
fALFF	−0.746 (0.225)[a]	−0.670 (0.240)[a]	0.248[b]0.019[c]	−0.6014 (0.231)[a]	−0.612 (0.221)[a]	0.868
ReHo	−0.726 (0.211)[a]	−0.548 (0.210)[a]	0.005[b]	−0.677 (0.289)[a]	−0.474 (0.174)[a]	0.004[b]

TLE:temporal lobe epilepsy. HC:healthy controls. fALFF: fractional amplitude of low-frequency fluctuations. ReHo, regional homogeneity. SUVR: standardized uptake value ratio. std, standard deviation. a: Significantly different from 0 by one sample t-test across subjects at $P < 0.05$. b: Significantly different between groups at $P < 0.05$, c: Significantly different between hemispheres in patients group at $P < 0.05$

back working-memory task.[9] These studies indicated a specific modulation effect of task-related activities between spontaneous neural activities and energy consumption. Consisted with these, our study found increased coupling between energy consumption and neural activity within gray matter in epilepsy.

Even so, the reason for the higher coupling between energy consumption and neural activity remains incompletely understood. We infer that neurometabolic decoupling might play a part in higher coupling. Previous studies have demonstrated that interictal discharges would result from an imbalance between neural excitatory and inhibitory activity.[23] Increased interictal glutamate levels also prove this point in mTLE-HS patients.[24] The astrocyte-neuron lactate shuttle makes a contribution to energy supply for neurons.[25] Although the detailed mechanisms mediating activity-dependent astrocyte-neuron energy delivery remains unknown, stronger neural activity would require more energy consumption in order to counterbalance the ATP-demand of the ion pump activity. Even in interictal epilepsy patients, elevated lactate levels were found, which might serve as a substrate for energy metabolism.[26] So higher coupling might be the modulating result for the strong hyperexcitability generated by epileptiform activity.

Neurovascular decoupling might be another possible explanation for the higher coupling. Altered coupling between metabolism and blood supply has been reported within the epileptic brain.[27] Epileptiform activity is found to be accompanied by strong extracellular potassium concentration,[28] although there may be a short time after abnormal discharge, where the brain is mildly ischemic until cerebrovascular autoregulation mechanisms works to increase blood flow. Eventually, high levels of extracellular potassium would adjust to an increase in blood flow, and then an increase in energy for neural activity. BOLD response is further changed by an overshooting supply of oxygenated hemoglobin from high increased blood flow.[29]

Our findings of a significant difference in the fALFF/SUVR coupling between Engel class IA and all others indicate that fALFF/SUVR coupling could predict seizure outcome after surgery. The predictive value of glucose metabolism in postoperative outcomes has been reported previously.[30] Class IA outcome was associated with a focal anteromesial temporal hypometabolism, while patients with surgical failure showed a mild temporal involvement sparing the hippocampus and relatively high extratemporal hypometabolism on both sides. Altered regional glucose metabolism was associated with postoperative outcomes. The lower the metabolism in the contralateral insula, the worse the outcome. While hypermetabolism in the right temporal pole was associated with a poor outcome. fALFF has been reported to estimate the epileptic activities and provide complementary functional information for disease diagnosis.[31] The fALFF/SUVR coupling may reflect the complementary functional information in the neurovascular structure. As modulation effects of task on the relationship between blood supply and functional activities, we speculated that higher fALFF/SUVR coupling might be a specific modulation effect of the epileptic activities. Seizures have been assumed to be typically a self-limiting phenomenon. Around the focal epileptic zone, an extensive inhibition would be generated to limit the propagation of discharges.[6] The higher fALFF/SUVR coupling might be the result of stronger inhibition, which indicates that the patients with higher correlation coefficient have stronger ability to control seizure in the brain by autoregulation. After standard anterior temporal lobectomy, they would be easily to have the less postoperative seizure. Patients with lower fALFF/SUVR coupling might have more disability in neurovascular structure. Previous study has confirmed that epilepsy patients with neurovascular lesions would have a limited seizure freedom.[32] Richard et al have also pointed out that supporting cellular bioenergetics and protecting neurovascular coupling may be promising therapeutic approaches.[29] So our findings suggested that fALFF/SUVR coupling has promise as adjuncts to help make an operative planning before surgery.

Several limitations in our study should be mentioned. First, a linear correlation index may simply present the complex and potential non-linear interactions between

spontaneous neural activities and energy consumption. More complex models are needed to assess these composite relationships in further researches. Second, most of patients were receiving anti-epileptic treatment during the imaging acquisition, which might have affected our results. It is not possible for patients to stop therapies because of ethical concerns. In fact, all patients have irregular seizures. Third, the sample size is small. We studied only 26 mTLE-HS. The study was underpowered to conclude altered bioenergetic coupling in all mTLE-HS and detect changes between left mTLE-HS and right mTLE-HS. Our study is a preliminary evidence suggesting that metabolic-functional correlations are disrupted in mTLE-HS. Therefore, a larger number of patients with wide ranges of epilepsy subtypes should be recruited in the future research. Meanwhile, the limited power to detect hemispherical differences would be overcome.

Conclusions

In summary, we revealed a high coupling between resting-state spontaneous neural activities and glucose metabolism in patients with mTLE-HS by using a simultaneous hybrid PET/MR scanner and its relationship with seizure outcomes. These findings suggest that the altered bioenergetic coupling may be a potential pathogenesis in mTLE-HS and would help make decision in surgical planning.

Acknowledgments

Conflict of Interests

The authors declared that they have no competing interests.

Authors' Contributions

JL and BCS conceptualized the study. YS and JDD analyzed and interpreted the patient data. BXC and KS did the statistical analysis. HWY and JJW wrote the manuscript and performed the imaging analysis. ZWC, JL, and GGZ revised the manuscript. All authors read and approved the final manuscript.

References

1. Bencurova P, Baloun J, Musilova K, et al. MicroRNA and mesial temporal lobe epilepsy with hippocampal sclerosis: whole miRNome profiling of human hippocampus. Epilepsia 2017;58:1782–1793.

2. Zou QH, Zhu CZ, Yang Y, et al. An improved approach to detection of amplitude of low-frequency fluctuation (ALFF) for resting-state fMRI: fractional ALFF. J Neurosci Methods 2008;172:137–141.

3. Zang Y, Jiang T, Lu Y, et al. Regional homogeneity approach to fMRI data analysis. NeuroImage 2004;22:394–400.

4. Zhang Z, Lu G, Zhong Y, et al. fMRI study of mesial temporal lobe epilepsy using amplitude of low-frequency fluctuation analysis. Hum Brain Mapp 2010;31:1851–1861.

5. Zeng H, Pizarro R, Nair VA, et al. Alterations in regional homogeneity of resting-state brain activity in mesial temporal lobe epilepsy. Epilepsia 2013;54:658–666.

6. Chassoux F, Artiges E, Semah F, et al. Determinants of brain metabolism changes in mesial temporal lobe epilepsy. Epilepsia 2016;57:907–919.

7. Leiva-Salinas C, Quigg M, Elias WJ, et al. Earlier seizure onset and longer epilepsy duration correlate with the degree of temporal hypometabolism in patients with mesial temporal lobe sclerosis. Epilepsy Res 2017;138:105–109.

8. Tomasi D, Wang GJ, Volkow ND. Energetic cost of brain functional connectivity. Proc Natl Acad Sci USA 2013;110:13642–13647.

9. Liang X, Zou Q, He Y, et al. Coupling of functional connectivity and regional cerebral blood flow reveals a physiological basis for network hubs of the human brain. Proc Natl Acad Sci USA 2013;110:1929–1934.

10. Khalili-Mahani N, van Osch MJ, de Rooij M, et al. Spatial heterogeneity of the relation between resting-state connectivity and blood flow: an important consideration for pharmacological studies. Hum Brain Mapp 2014;35:929–942.

11. Aiello M, Cavaliere C, Salvatore M. Hybrid PET/MR imaging and brain connectivity. Frontiers in neuroscience 2016;10:64.

12. Nugent AC, Martinez A, D'Alfonso A, et al. The relationship between glucose metabolism, resting-state fMRI BOLD signal, and GABAA-binding potential: a preliminary study in healthy subjects and those with temporal lobe epilepsy. J Cereb Blood Flow Metab 2015;35:583–591.

13. Marchitelli R, Aiello M, Cachia A, et al. Simultaneous resting-state FDG-PET/fMRI in Alzheimer Disease: relationship between glucose metabolism and intrinsic activity. NeuroImage 2018;176:246–258.

14. Blumcke I, Thom M, Aronica E, et al. International consensus classification of hippocampal sclerosis in

temporal lobe epilepsy: a Task Force report from the ILAE Commission on Diagnostic Methods. Epilepsia 2013;54:1315–1329.

15. Engel J. Update on surgical treatment of the epilepsies: Summary of The Second International Palm Desert Conference on the Surgical Treatment of the Epilepsies (1992). Neurology 1993;43(8):1612.

16. Gonzalez-Escamilla G, Lange C, Teipel S, et al. PETPVE12: an SPM toolbox for Partial Volume Effects correction in brain PET - Application to amyloid imaging with AV45-PET. NeuroImage 2017;147:669–677.

17. Yan CG, Wang XD, Zuo XN, et al. DPABI: data processing & analysis for (resting-state) brain imaging. Neuroinformatics 2016;14:339–351.

18. Zijlmans M, Zweiphenning W, van Klink N. Changing concepts in presurgical assessment for epilepsy surgery. Nat Rev Neurol 2019;15:594–606.

19. Vielhaber S, Niessen HG, Debska-Vielhaber G, et al. Subfield-specific loss of hippocampal N-acetyl aspartate in temporal lobe epilepsy. Epilepsia 2008;49:40–50.

20. Aiello M, Salvatore E, Cachia A, et al. Relationship between simultaneously acquired resting-state regional cerebral glucose metabolism and functional MRI: a PET/MR hybrid scanner study. NeuroImage 2015;113:111–121.

21. Riedl V, Bienkowska K, Strobel C, et al. Local activity determines functional connectivity in the resting human brain: a simultaneous FDG-PET/fMRI study. J Neurosci 2014;34:6260–6266.

22. Hahn A, Gryglewski G, Nics L, et al. Task-relevant brain networks identified with simultaneous PET/MR imaging of metabolism and connectivity. Brain Structure Function 2018;223:1369–1378.

23. Du R, Zhu X, Wu S, et al. PET imaging of metabolic changes after neural stem cells and GABA progenitor cells transplantation in a rat model of temporal lobe epilepsy. Eur J Nucl Med Mol Imaging 2019;46:2392–2397.

24. Barker-Haliski M, White HS. Glutamatergic mechanisms associated with seizures and epilepsy. Cold Spring Harb Perspect Med 2015;5:a022863.

25. Boison D, Steinhauser C. Epilepsy and astrocyte energy metabolism. Glia 2018;66:1235–1243.

26. Angamo EA, ul Haq R, Rösner J, et al. Contribution of intrinsic lactate to maintenance of seizure activity in neocortical slices from patients with temporal lobe epilepsy and in rat entorhinal cortex. Int J Mol Sci 2017;18(9):1835.

27. Song Y, Torres RA, Garcia S, et al. Dysfunction of neurovascular/metabolic coupling in chronic focal epilepsy. IEEE Trans Biomed Eng 2016;63:97–110.

28. Rassner MP, Moser A, Follo M, et al. Neocortical GABA release at high intracellular sodium and low extracellular calcium: an anti-seizure mechanism. J Neurochem 2016;137:177–189.

29. Kovacs R, Gerevich Z, Friedman A, et al. Bioenergetic mechanisms of seizure control. Front Cell Neurosci 2018;12:335.

30. Chassoux F, Artiges E, Semah F, et al. (18)F-FDG-PET patterns of surgical success and failure in mesial temporal lobe epilepsy. Neurology 2017;88:1045–1053.

31. Reyes A, Thesen T, Wang X, et al. Resting-state functional MRI distinguishes temporal lobe epilepsy subtypes. Epilepsia 2016;57:1475–1484.

32. Kassiri J, Rajapakse T, Wheatley M, et al. Neurovascular lesions in pediatric epilepsy. J Child Neurol 2019;34:549–555.

Supporting Information

Additional supporting information may be found online in the Supporting Information section at the end of the article.

Supplementary Figure S1. Gray matter volume in bilateral hippocampi was estimated. (A) Regions of interest chose as seed region in the right and left hippocampi; (B) Average voxel-based morphometry revealed significant gray matter atrophy of ipsilateral hippocampus in patients group, while no significant differences showed in contralateral hippocampus.